3rd International Conference on Automation, Control, Engineering and Computer Science (ACECS'16)
Proceedings of Engineering & Technology (PET)
pp. 245-251

Development of electrical discharges in water: application for electrical fracturing of shale gas

Henda Jabberi[#1], Faouzi Ben Ammar[#2]

[#]*Laboratoire de Recherche Matériaux, Mesures et Applications,*
Institut National des Sciences Appliquées et de Technologie INSAT

[1]jabberi.henda@gmail.com

[2]faouzi.benamar@yahoo.fr

***Abstract*— Discharges inside water have been widely used for pulsed power applications such as rock fragmentation. Shock wave generators are important tool for generation a high voltage wave between inter-electrodes space. This paper reviews development of electrical discharge in water to optimize the electrical fracturing process. In the context, the authors propose a recent structure for electrical fracturing process based on Marx generator. This structure ensures the discharges in subsonic mode. As a result, an appropriate model of electrical fracturing devise and inter-electrodes space are achieved.**

***Keywords—electrical discharge in water;* shock waves; shale gas; Marx generator; subsonic disharge;**

I. INTRODUCTION

Recent research in pulse power technology has opened up a wide range of potential applications [1], such as medicine, material processing, biological studies, manufacturing, and geophysical studies. Electrically produced shock waves can also be generated in water as a means of rock fragmentation [2, 3].

Many studies were processed in order to investigate the potential of electric fracturing for shale gas reserves. In accordance with Leon [4], the pressure wave characteristic should be controlled to generate an acoustic wave and not a shock wave. Mao [5] presents experimental results of electrical fracturing rocks submitted to various tri-axial constraints. The length of the fractures was studied for energies of the order of kilojoules and dynamic pressures up to 50MPa. This process generates multiple radial fractures whose number and length depend on the mechanical characteristics of the rock. According to Cho [6], the form of the dynamic pressure wave has a great importance on the type of fracture. More specifically, the rise time of the pressure pulse has a significant effect on the diffuse fracture appearance. The more frequency spectrum of the wave is high frequency, the more damage is diffused but weakly penetrating. Chen [7] presents the characterization of the damage rock based only on the amplitude of the pressure wave (single or repetitive shocks) and levels of static constraints applied. The permeability increases with the maximum pressure level, whatever the level of containment. However, there is a threshold effect of the permeability as a function of the pressure level, which depends on the level of containment [8]. On other hand, Martin studies the influence of all parameters related to the discharge circuit in order to control the phenomenology of the discharge in the fluid, and consequently fully control the amplitude and dynamics pressure wave [9].

The process of the electric fracturing for shale gas is shown in Fig.1. The electrode system connected to an electric power source is immersed in water (d is the inter-electrode distance) and D is the distance between the arc generated and shale rock.

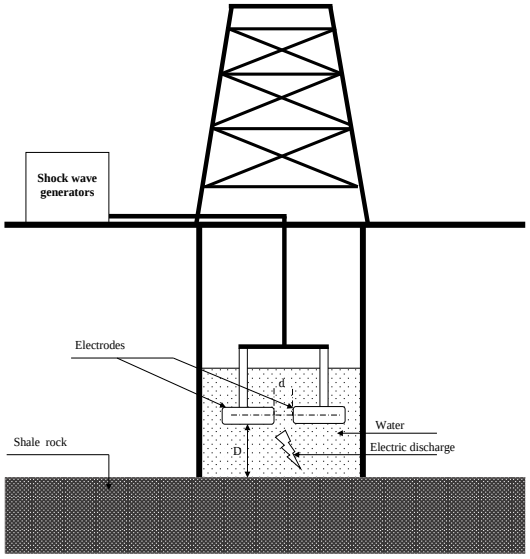

Fig. 1 Electrical fracturing process of shale gas.

Among the methods of a high-amplitude wave generation, there is the electrical discharge technique in the water, which occurs between two electrodes. In the first phase, an application of a high-voltage (HV) pulse leads to an electrical breakdown between a pair of electrodes and a development of a growing streamer, which subsequently connects both electrodes. In the second phase, further energy deposition into the formed spark leads to its explosive expansion in the radial direction and the generation of the shock wave in the surrounding liquid [10].

The main objective of this paper is to generate high pulsing voltage discharge in water to optimize the electrical fracturing process of shale gas. Shock waves have been generated by

ISSN: 2356-5608

electrical discharges in water in subsonic mode. This study of development of pulsed arc electrohydraulic discharge allows optimizing the conversion of electrical energy into acoustic energy.

II. System description and modeling of electrical discharges in water

The phenomena of dielectric breakdown can be divided into two phases when a high voltage waveform is applied to water. The time between the application of the wave voltage and the priming of the electric arc corresponds to the pre-breakdown phase [t=0, t=T_b [. The time of setting a short circuit by apparition the electric arc using the inter-electrodes device immersed in water presents the post-breakdown phase [t=T_b, t].

For the generation of electric arc, the authors propose a Marx generator with peak amplitude of 50 kV, the rise time is about 3 µs and fall time can reach several tens of microseconds.

The Marx generator concept, as shown in Fig. 2, charging capacitors (C_1 to C_5) in parallel (through resistive charging elements, R) and discharging them in series into the load (through switches, g), provides another widely used method for generating high-voltage pulses, because it requires only a relatively low-voltage power supply, (V_{in}=10 kV), for charging and does not require pulse transformers to achieve the desired high-voltage [11].

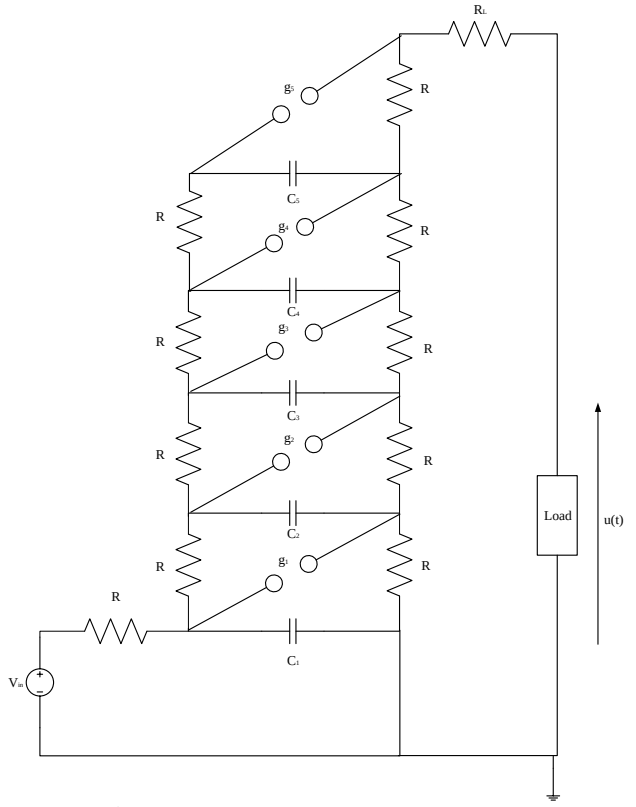

Fig. 2 Basic five stages Marx generator topology.

Consider the design of a five stage Marx generator with 10 kV charging. The simulated result is shown in Fig. 3.

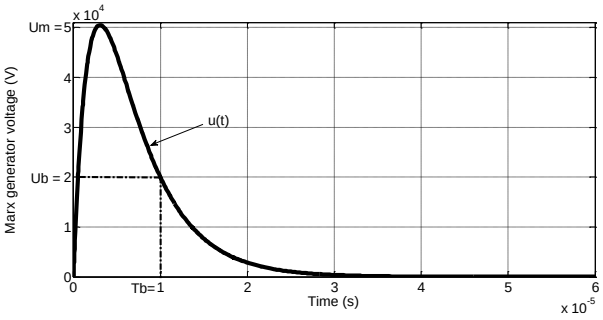

Fig. 3 Marx generator output voltage.

The electric parameters, which characterize the voltage waveform until the water gap breakdown, are:

- Maximum charging voltage U_m;
- Delay time to breakdown T_b;
- Voltage value U_b at the breakdown time T_b.

In the first phase and for a subsonic discharge mode, the application of long duration high voltage pulse between a pair of electrodes leads to the development of bubbles where the gas discharge take place. Moreover, the pulsed electrical arc discharges are associated with the emission of a power shock wave propagating radially into water. Fig .4 explains the process of wave propagation in water gap.

A. Pre-breakdown phase

For a subsonic discharge mode, pre-breakdown phase is both the seat of thermal effects (gas bubbles) and electrical effects (propagation of the discharge in the bubbles). If the energy input is sufficient to create a volume of gas occupying the entire inter-electrode space, so the breakdown of the gap may intervene. Depending on the configuration, the geometry of which involves electrodes, the inter-electrode distance, the water conductivity and its parameters thermodynamic, it is clear that the amount of heat energy required for vaporization of the water volume between the two electrodes will be different.

The authors propose an equivalent circuit diagram for pre-breakdown phase, which is represented by Fig. 5.

When the capacitor of Marx generator C is charged to the desired voltage U_m, a trigger pulse is used to control the switch. A circuit impedance $Z_{circuit}$ associated in series with the global water impedance Z_{water} can model this discharge.

The circuit impedance $Z_{circuit}$ includes the equivalent inductance of the set of elements inductive denoted $L_{circuit}$ placed in series with the equivalent resistance to all resistive elements denoted $R_{circuit}$.

During the pre-breakdown phase, the overall impedance Z_{water} between the inter-electrodes space can be modeled the water resistance R_{water} parallel water capacitance C_{water}. The value of the inter-electrode resistance R_{water} depends on several parameters: the inter-electrode configuration (inter-electrode distance and geometry), the geometry of the containment, the initial conductivity of the water, the water temperature

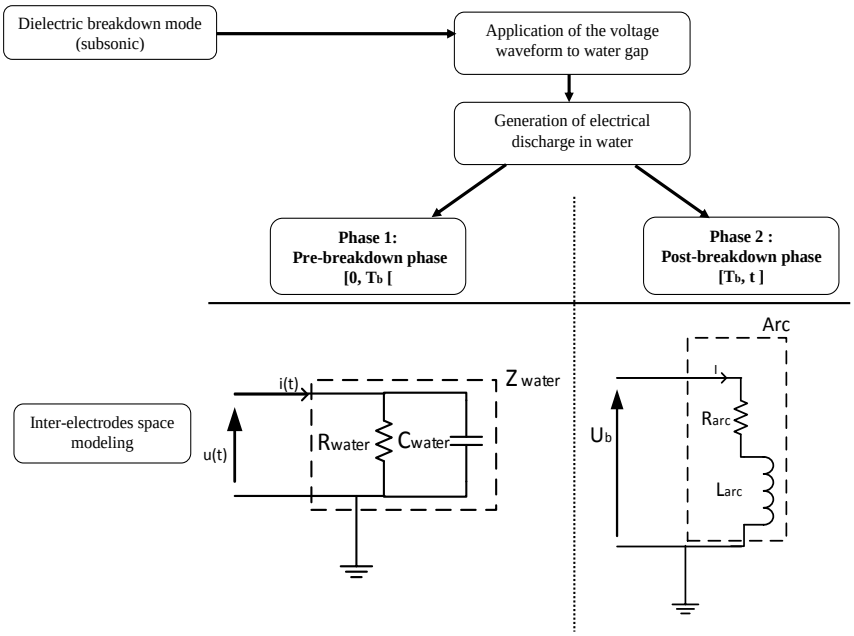

Fig. 4 Process of the wave propagation in water.

The value of water resistance R_{water} can vary from a few hundred Ohms to a few kilo Ohms. We can note that the water resistance is significantly higher than the electrical circuit resistance $R_{circuit}$. Consequently, we can consider that the value of the overall resistance of the circuit, in the pre-breakdown phase is equal to R_{water}. [12]

The equivalent capacitance C_{water} is determined using (1).

$$C_{water} = \frac{\varepsilon_0 \varepsilon_r S}{d} \quad (1)$$

Where, ε_0 is permittivity of vacuum (8.854187 10^{-12} F/m), ε_r is relative permittivity of the dielectric, S is the electrode surface and d is inter-electrode distance.

The values of the equivalent capacity C_{water} is in order of hundreds of pF. The capacitance values C used are always important to this equivalent capacity. The influence of C_{water} is negligible [12].

The simulation results are modeled with R_{water}=96 Ω and C_{water}= 110 pF.

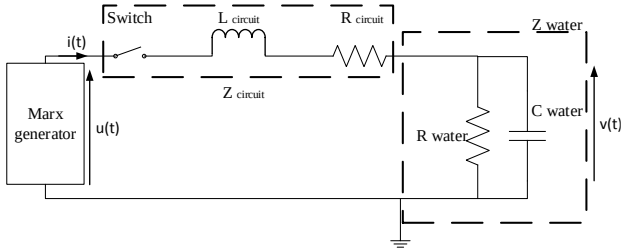

Fig. 5 Equivalent electrical circuit during pre-breakdown phase.

From the equivalent circuit of the pre-breakdown phase, expression of the current i(t), the voltage v(t) and the power P(t) can be modeled as follows:

$$i(t) = \frac{U_m}{R_{water}} \left\{ \exp\left(-\frac{R_{water}}{L_{circuit}} t \right) - \exp\left(-\frac{1}{R_{water} C} t \right) \right\} \quad (2)$$

$$v(t) = U_m \left\{ \exp\left(-\frac{R_{water}}{L_{circuit}} t \right) - \exp\left(-\frac{1}{R_{water} C} t \right) \right\} \quad (3)$$

$$P(t) = \frac{U_m^2}{R_{water}} \left\{ \exp\left(-\frac{R_{water}}{L_{circuit}} t \right) - \exp\left(-\frac{1}{R_{water} C} t \right) \right\}^2 \quad (4)$$

Between the instants t = 0 and t = T_b (with T_b is the breakdown time), it is possible to define the energy during the pre-breakdown phase by:

$$E_c = \int_0^{T_b} p(t).dt = \frac{1}{R_{water}} \int_0^{T_b} v^2(t).dt \quad (5)$$

$$E_c = \frac{1}{2} C.U_m^2 \left[1 - \exp\left(\frac{-2T_b}{R_{water} C} \right) \right] \quad (6)$$

The energy is a function of the value of the voltage U_m of Marx generator C, the value of the equivalent resistance of the inter-electrode space R_{water} and the breakdown time T_b.

B. Post-breakdown phase

The second phase is the post-breakdown phase. The time origin of this phase corresponds to the time of setting a short circuit, by establishing the electric arc with the inter-electrode device immersed in water. The formation of this arc allows a rapid transfer of energy to the fluid, which leads to the initiation of the pressure wave and its propagation in the water. The authors propose an equivalent circuit diagram for the post-breakdown phase, which is represented by the simplified circuit as shown in Fig. 6.

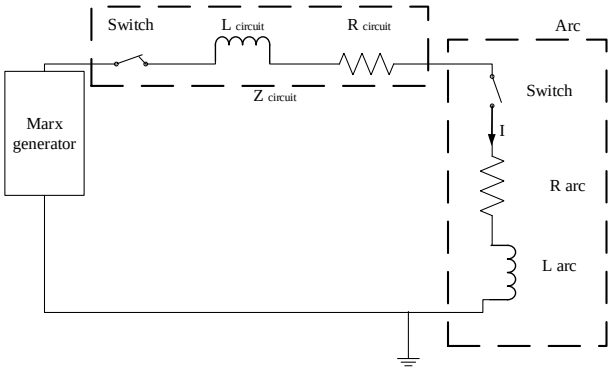

Fig. 6 Equivalent electrical circuit during post-breakdown phase.

During the post-breakdown phase, the overall impedance between the electrodes can be modeled by Z_{arc} (comprises a resistance R_{arc} and a series inductor L_{arc}).

Different equations allow to determine the value of $r_{arc}(t)$ [13-16]. Timoshkin [17] proposed another expression of the value of $r_{arc}(t)$ according to formula (7).

$$r_{arc}(t) = \frac{\alpha_s d}{\sqrt{\int i^2(t)dt}} \tag{7}$$

Where, α_s represents the normalized arc time constant to the electric discharge.

In accordance with Timoshkin [17] and Mackersie [18], the value of R_{arc} is based on the maximum values current switched. R_{arc} is between 20mΩ and 200mΩ.

The evolution of the discharge channel over time also causes an evolution of the arc inductance. The L_{arc} value can be approximated by considering the inductance per unit length of a coaxial guide (Formula (8)) [19].

$$l_{arc}(t) = l\frac{\mu_0}{2\pi}\ln\left(\frac{r_c}{r_s(t)}\right) \tag{8}$$

Where, l is the length of inter-electrodes space, r_c is the external radius and $r_s(t)$ is the variation over time of the radius of the discharge channel. The values of the inductance arc obtained using (8) are about several tens of nanohenries per millimeter. These values are negligible compared to the circuit inductance $L_{circuit}$.

In the next section, the simulation results are modeled with R_{arc}=170 mΩ and L_{arc} = 10 nH.

At the time of short-circuit of the inter-electrode space, the Marx generator capacitor is charged to the residual voltage U_b. It follows a discharge of this capacity in the circuit modeled by the circuit impedance $Z_{circuit}$ coupled in series with the overall arc impedance (R_{arc} and L_{arc}). The circuit impedance is similar to that presented in fig. 5. It is composed of two serial elements: the inductance $L_{circuit}$ and the resistance $R_{circuit}$.

The current i (t) during the breakdown and the post-breakdown phases can be expressed by:

$$i(t) = U_b\sqrt{\frac{C}{L_{circuit}}}\exp\left(-\frac{R}{2L_{circuit}}t\right)\sin\left(\omega_n t\right) \tag{9}$$

Where, $R = R_{arc} + R_{circuit}$ and $\omega_n = \sqrt{\frac{1}{L_{circuit}C}}$

The parameters L, C and R are respectively, the inductance, the capacity and the resistance of the equivalent circuit.

According to the expression of the current flowing in the circuit during the pre-breakdown phase, the electrical power of the arc is expressed by:

$$P_{arc}(t) = R_{arc}U_b^2\frac{C}{L_{circuit}}\exp\left(-\frac{R}{L_{circuit}}t\right)\sin^2\left(\omega_n t\right) \tag{10}$$

The maximum value $I_{max} = i(T_{max})$ of the discharge current injected into the arc channel is given by:

$$I_{max} = U_b\sqrt{\frac{C}{L_{circuit}}}\exp\left(-\frac{R}{2L_{circuit}}T_{max}\right)\sin\left(\omega_n T_{max}\right) \tag{11}$$

I_{max} current is expressed by (12).

$$I_{max} = U_b\sqrt{\frac{C}{L_{circuit}}}\exp\left(-\frac{R\pi}{4}\sqrt{\frac{C}{L_{circuit}}}\right) \tag{12}$$

We can also express I_{max} in function of the energy E_b available upon breakdown by:

$$E_b = \frac{1}{2}CU_b^2 \tag{13}$$

With U_b as the voltage remaining at the breakdown time.

$$I_{max} = \sqrt{\frac{2E_b}{L_{circuit}}}\exp\left(-\frac{R\pi}{4}\sqrt{\frac{C}{L_{circuit}}}\right) \tag{14}$$

III. Results and Discussion

We propose in this paper an equivalent circuit diagram for pre-breakdown, breakdown and post-breakdown phases using the Marx generator as a power supply with peak amplitude of 50 kV. According to Fig. 7 and Table 1, the authors propose a reconfigurable equivalent electric model. The switches MS1, MS2, MS3, and MS4 are able to describe the three pre-breakdown, breakdown and post-breakdown phases.

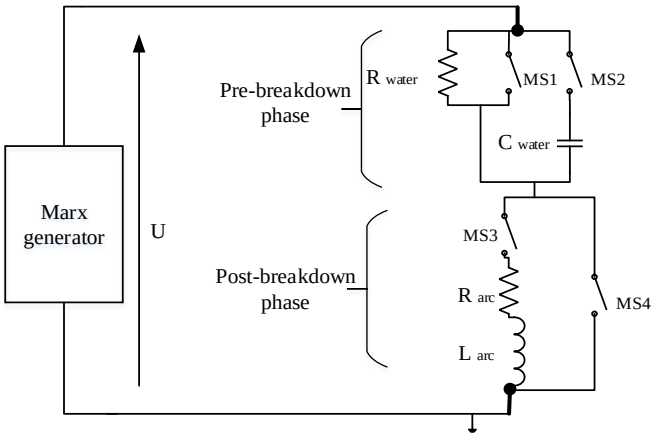

Fig. 7 Equivalent electrical circuit for pre-breakdown, breakdown and post-breakdown phases.

TABLE I
CONFIGURABILITY OF INTER-ELECTRODES SPACE

Phases	**MS1**	**MS2**	**MS3**	**MS4**
Pre-breakdown	0	1	0	1
Breakdown	1	0	1	0
Post-breakdown	1	0	1	0

The simulation result in MATLAB Simulink of the voltage between inter-electrodes space, the current crossing inter-electrodes space, the power between inter-electrodes space and a typical set of results is shown in Fig. 8.

The simulation results are modeled with $R_{circuit}$ = 0.17Ω and $L_{circuit}$=1.7 µH.

The pre-breakdown phenomena duration is about 10 µs. During this period, ionic conduction through the water to ground takes place. The current associated with pre-breakdown phenomena is not visible with regard to the scale of the Fig. 8. Nevertheless, this pre-breakdown current is easily measurable. It is of the order of 525 A and leads to a voltage decrease of about 60%.

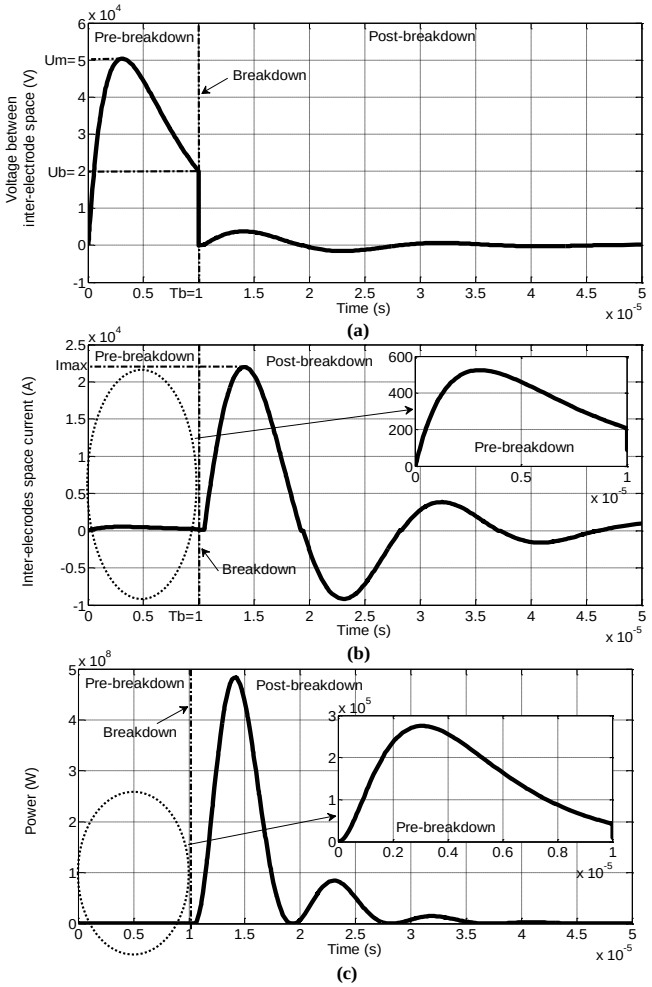

Fig.8 (a) Output voltage between inter-electrodes space, (b) inter-electrodes space current, (c) Power between inter-electrodes space.

At breakdown time T_b, the current peak reaches 22 kA and then produces an oscillatory current discharge. This oscillatory shape is due to the capacitor of Marx generator through the equivalent circuit inductance $L_{circuit}$ in series with the spark channel equivalent inductance L_{arc} and resistance R.

The amplitude of the wave is defined as a function of the electrical energy available upon breakdown E_b, and the distance between the electrodes and the surface. All the results using the empirical law that determines the value of the amplitude of the pressure wave as a function of electric power Eb available when the arc appears [20].

$$P_{\max} = \frac{9000}{r} E_b^{\alpha} \tag{14}$$

Where, P_{max} is the peak pressure (bar), r is the distance between the arc and the sensor (mm), α is a coefficient depending on the geometry of the inter-electrode device.

In accordance with [9], the expression of the pressure can be expressed by:

$$P_{\max} = k_1 I_{\max} \tag{15}$$

With k_1 is a function of the distance between the inter-electrodes space and the breakdown mode.

IV. CONCLUSION

Shock waves have been generated by a Marx generator power supply enabling subsonic discharge in water. The particularity of the Marx generator is to provide the both discharge modes (subsonic and supersonic). The pre-breakdown phase corresponds to the time duration that the stored electrical energy is transferred to the fluid and converted into thermal energy to permit vaporization of the water volume located between the electrodes space.

During the pre-breakdown phase, the equivalent resistance of the inter-electrode device depends on both the geometry of the device, the physical properties (conductivity) and thermodynamic fluid (temperature). Post-breakdown phase corresponds to the brutal transfer of electrical energy available to the arc. This phase is essential, because it allows generating the shock wave.

An equivalent circuit model for both pre-breakdown phase and post-breakdown phase has been proposed. It simulates the time evolutions of the electrical quantities (current, voltage and power) as well as of the energy consumed.

REFERENCES

[1] Levy S, Nikolich M, Alexeff I, Rader M, Buttram MT and Sarjeant W J. Commercial applications for modulators and pulsed power technology Proc. 20th Power Modulator Symp. (Myrtle Beach, CA), pp. 8–15, 1992.

[2] Proko S, Schofield G, Hamelin M and Kitzinger F. Proc. 9th IEEE Int. Pulsed Power Conf. (Albuquerque), 1993.

[3] Weise T, Hofmann J and Loffler M. Proc. 10th IEEE Int. Pulsed Power Conf. (Albuquerque, NM), 1995.

[4] J. F. LEON and J. FRAM. Pulse Fracturing Device and Method. U.S. Patent US20070004773P 2007113007, 2011.

[5] R. Mao, H. De Pater, J. F. Leon, J. Fram, R. Ewy, S. Storslett, and J. Stefani. Experiments on Pulse Power Fracturing. 2012.

[6] S. Ho Cho and K. Kaneko. Influence of the applied pressure waveform on the dynamic fracture processes in rock. International Journal of Rock Mechanics and Mining Sciences, vol. 41, no. 5, pp. 771–784, 2004.

[7] W. CHEN. Fracturation électrique des géomatériaux: Etude de l'endommagement et de la perméabilité. Thèse de doctorat, Université de Pau et des Pays de l'Adour,Pau, 2010.

[8] W. Chen, O. Maurel, T. Reess, A. S. De Ferron, C. La Borderie, G. Pijaudier Cabot, F. Rey Bethbeder, and A. Jacques. Experimental study on an alternative oil stimulation technique for tight gas reservoirs based on dynamic shock waves generated by Pulsed Arc Electrohydraulic Discharges. Journal of Petroleum Science and Engineering, vol. 88–89, pp. 67–74, 2012.

[9] J. Martin, T. Reess, A. De Ferron, F. Rey-Bethbeber, A. Jacques, O. Maurel, C. La Borderie, G. Pijaudier-Cabot, A. Gibert. Electrical and Static fracturing of a reservoir. Fr. Patent, WO/2012/123461, 2012.

[10] V. Stelmashuk and P. Hoffer. Shock Waves Generated by an Electrical Discharge on Composite Electrode Immersed in Water With Different Conductivities. IEEE TRANSACTIONS ON PLASMA SCIENCE, VOL. 40, NO. 7, 2012.

[11] Willis, W. L.: "Pulse-Voltage Circuits", Chapter 3 de "High Power electronics", Editor Dollinger, R. E.; Sarjeant, W. James, Tab Books Inc., 1st Edition, 1989, ISBN 0-8306-9094-8.

[12] M. Justin. Etude et caractérisation d'onde de pression générée par une décharge électrique dans l'eau. Application à la fracturation électrique des géomatériaux. Thèse de doctorat, Université de Pau et des Pays de l'Adour,Pau, 2013.

[13] M. TOEPLER. Zur Bestimmung der Funkenkonstante. Archiv f. Elektrotechnik, vol. 18, no. 6, pp. 549–562, 1927.

[14] S. I. BRAGINSKII. Therory of development of a spark channel. Sov. Phys. JETP, vol. Bb. 7, pp. 1068–1074, 1958.

[15] T. H. Martin, M. Williams, and M. Kristiansen, J.C. Martin. Pulsed Power. Springer, 1996.

[16] I. V. Timoshkin. electrical disintegartion of ores and slags and liberation of valuable inclusions. University of London and the Diploma Of Imperial College, 2001.

[17] I. V. Timoshkin, R. A. Fouracre, M. J. Given, and S. J. Macgregor. Hydrodynamic modelling of transient cavities in fluids generated by high voltage spark discharges. J. Phys. D: Appl. Phys., vol. 39, no. 22, pp. 4808–4817, Nov. 2006.

[18] J. W. Mackersie, I. V. Timoshkin, and S. J. Macgregor. Generation of high-power ultrasound by spark discharges in water. IEEE Transactions on Plasma Science, vol. 33, no. 5, pp. 1715–1724, Oct. 2005.

[19] M. J. Kushner, W. D. Kimura, and S. R. Byron. Arc resistance of laser-triggered spark gaps. Journal of applied physics, vol. 58, no. 5, pp. 1744–1751.

[20] G. TOUYA, T. REESS, L. PECASTAING, A. GIBERT, and P. DOMENS, "Development of subsonic electrical discharges in water and measurements of the associated pressure waves," J. Phys. D: Appl. Phys., vol. 39, no. 24, pp. 5236–5244, 2006.